

- [2] Rother C, et al., Grabcut: Interactive foreground extraction using iterated graph cuts, *ACM TOG*, 23(3): pp.309–314, 2004.
- [3] Boykov Y, et al., Fast Approximate Energy Minimization via Graph Cuts, In *ICCV*, 1, pp.377–384, 1999.
- [4] Xiao D, et al., 3D detection and extraction of bladder tumors via MR virtual cystoscopy, *Int. J. CARS*, pp. 1–8, 2015.

Improving soft tissue segmentation in CT volumes using a sigmoid-based active shape model

Mina Esfandiarkhani¹, Amir Hossein Foruzan¹, Yen-Wei Chen²

¹Department of Biomedical Engineering, Engineering Faculty, Shahed University, Tehran, Iran

²Intelligent Image Processing Lab, College of Information Science and Engineering, Ritsumeikan University, Shiga, Japan

Keywords Active shape model · Sigmoid edge model · Liver segmentation · Medical image processing.

Purpose

The success of Active Shape Models is largely dependent on accurate assignment of point correspondences. Improper labeling of shape points results in unsmooth shape and inaccurate appearance models. This point is vital especially in segmentation of soft tissues with large shape variations. We propose a generalized edge model and employ it in the search algorithm to improve segmentation of liver in the presence of noise and Partial Volume Effect (PVE). Also, we tackle constraints imposed by Gaussian intensity profiles in the conventional ASM [1]. Sigmoid function is used to model the gray-level profiles and classify shape points into genuine and dubious groups.

Methods

We employ the “Narrow Band Thresholding” technique [2] to initially segment the liver. Initial boundary of a slice is represented by a set of points. In order to speed up our algorithm, the number of points is reduced based on their distance and curvature. We reduce number of points in low-curvature regions of the contour. Next, intensity profiles are sampled along the normal vector in each point. An intensity profile is modeled by a sigmoid function and the parameters of the model are used to estimate the location of the bordering point. Based on the quality of model fitness which is measured quantitatively, we assign a confidence weight to a point representing how well a sigmoid function fits the current profile. If the quality of fitness is below a threshold, the point will be labeled as a dubious point. It means that the boundary point is not located on a strong edge (due to partial volume effect or noise). Thereby, boundary points are clustered into true and false boundary points.

Using the position of true boundary points (genuine points), we estimate the position of false boundary points through fitting a cubic Smooth Spline [3]. To improve the results, we employ a statistical shape model and constrain the shape by the model.

Results

We applied our method to two different CT datasets. The first dataset belonged to Osaka University Hospital, Japan. It contained 30 abnormal abdominal CT images of the second phase with a resolution and size of $512 \times 512 \times 159$ and $0.63 \times 0.63 \times 1.25$ mm³, respectively. The second set included 20 liver CT images of MICCAI 2007 Grand Challenge (Fig. 1).

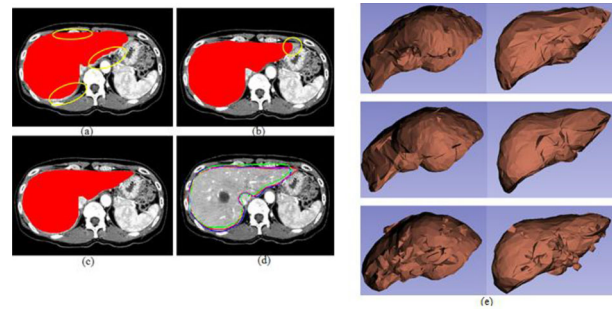


Fig. 1 Typical visualizations of our results. Segmented livers by (a) conventional ASM, (b) proposed method and (c) gold standard. (d) Boundaries of conventional ASM (green), proposed method (blue) and gold standard (red) in a typical slice. (e) Surface rendering of two typical livers. Left column: Osaka dataset, no. 2. Right column: MICCAI dataset, no. 4. Rows from top to bottom: The proposed, manual and Active Contour Model results

We evaluated the proposed method using Dice, Jaccard and MICCAI 2007 Grand Challenge metrics [4]. Quantitative evaluations of our method for both groups are given in Table 1.

Table 1 Quantitative evaluations of our results

Dataset	Signed Rel. Vol. Diff. [%]	Avg. Sym. Surf. Dist. [mm]	Avg. Sym. RMS Surf. Dist. [mm]	Max Surf. Dist. [mm]	Vol. Overlap Err. [%]
Osaka	-0.75	1.85	3.01	21.56	12.1
MICCAI training dataset	-0.09	1.82	3.61	30.12	10.29

The average Dice (Jaccard) metrics are 0.93 (0.87) and 0.94 (0.89) for the 1st and 2nd dataset, respectively. The indices are 0.88(0.76) and 0.85 (0.73) for Active Contour Model (ACM), conventional ASM, respectively. The results are improved at least 0.05 and 0.08 with respect to conventional ASM and ACM methods.

Conclusion

We proposed a generalized edge model which alleviates problems concerned with profile modeling and inaccurate point correspondences in the ASM algorithm. It is robust to noise and PVE and does not leakage to nearby organs. In future, we decide to dynamically change the threshold of genuine and dubious landmarks selection.

References

- [1] Cootes, T.F., Taylor, C.J., D.H. Cooper and Graham, J., “Active shape models—their training and application,” *Computer Vision and Image Understanding*, 61(1), pp. 38–59, Jan. 1995.
- [2] Foruzan, A. H., Yen-Wei, C. H. E. N., Zoroofi, R. A., Furukawa, A., Masatoshi, H. O. R. I. and TOMIYAMA, N. (2013).

Segmentation of liver in low-contrast images using K-means clustering and geodesic active contour algorithms. *IEICE TRANSACTIONS on Information and Systems*, 96(4), 798–807.

- [3] Härdle, W. and Linton, O. (1994). Applied nonparametric methods. *Handbook of econometrics*, 4, pp. 2295–2339.
- [4] Van Ginneken, B., Heimann, T. and Styner, M. (2007). 3D segmentation in the clinic: A grand challenge. *3D segmentation in the clinic: a grand challenge*, pp. 7–15.

Supervised Hessian-based vessels segmentation in narrow-band laryngeal images

S. Moccia^{1,2}, E. De Momi², A. Ghilardi², A. Lad², L. S. Mattos¹

¹Istituto Italiano di Tecnologia, Department of Advanced Robotics, Genova, Italy

²Politecnico di Milano, Department of Electronics, Information and Bioengineering, Milano, Italy

Keywords Narrow-band laryngoscopy · Laryngeal tumor · Vesselness measure · Supervised vessel segmentation

Purpose

The stage in which a laryngeal tumor is diagnosed has strongly impact on patients' mortality or after treatment morbidity. The current diagnosis practice requires sampling suspicious laryngeal tissue, identified through endoscopic examination, for subsequent histopathological analysis. During the endoscopy, clinicians mainly focus on identifying vascular pattern modifications, which are well known to correlate to cancer onset.

Recent developments in this field have led to the introduction of narrow-band (NB) endoscopy. NB enhances the visualization of superficial vessels, thus improving the detection of tumors, especially at early stages, when the diagnosis is challenging but crucial for the patient [1].

In this context, a computer-assisted scheme has the potential to greatly improve tissue evaluation during the diagnosis, increasing the efficiency in managing patients and leading to potentially enormous benefits, especially resulting from an improved detection of early tumors, which may pass unnoticed to the human eye.

Methods

The proposed method consists in three main steps: (i) Pre-processing, (ii) Vessel enhancement and (iii) Vessel segmentation.

The pre-processing step concerns noise suppression, mainly associated to CMOS and CCD image sensors, and edge enhancement. In this work, a non-linear anisotropic rotation invariant diffusion scheme [2] was used. The key idea is to smooth non-informative homogeneous areas with an isotropic Gaussian-like kernel and enhance meaningful edges by an anisotropic kernel, elongated in the direction parallel to the edge itself. The two eigenvectors of the structure tensor \mathbf{J} were employed to estimate the edges direction, while the amount of diffusion was defined by a combination of \mathbf{J} eigenvalues, defined to preserve both plate-like and tubular-like structure.

A second issue is related to the presence of specular reflections (SR), due to the strong illumination of the endoscope and the wet and smooth surface of laryngeal tissue. SR have to be identified and masked, since they represent a source of errors for the vessel segmentation algorithm. SR segmentation was performed with a thresholding scheme on both the saturation (low for SR) and brightness (high for SR). The two thresholds were set as the best compromise between sensitivity and specificity after a receiver operative characteristic (ROC) curve analysis.

The vessel enhancement was performed with the image Hessian eigenvalues (λ_1, λ_2 with $|\lambda_1| \leq |\lambda_2|$) analysis. \mathbf{H} was computed

according to the scale-space theory [3], namely convolving the image with the second partial derivatives of a Gaussian kernel with scale σ . Since laryngeal vessels can assume both healthy tubular-like ($|\lambda_1| \ll |\lambda_2|$) and pathological blob-like ($|\lambda_1| \approx |\lambda_2|$) structure, only the amplitude of λ_2 was considered. Moreover, only negative λ_2 were retained because vessels in NB images are darker than the background. Different σ values were considered to take in account for vessels with different thickness, resulting in a multi-scale framework analysis.

The multi-scale vesselness measures computed in the previous step were used as input features to a linear support vector machine (SVM) classifier to obtain vasculature segmentation. The input features were normalized to obtain variables with zero-mean and unit standard deviation, according to the approach in [4]. Two classes have been considered during the classification process: vessel and background class. Through this classification of pixels, the final vessels segmentation was achieved.

Results

A dataset of twenty pathological NB laryngeal frames was used in this research, with an image size of 478x311 pixels. Ten images were used to tune the algorithm parameters and train the SVM, while the remaining ten were used to test the proposed algorithm performance with respect to gold-standard manual segmentations performed by an expert. The adopted metrics were the area under the ROC curve for the enhancement step, and accuracy, sensitivity and specificity for the segmentation step. The proposed approach performed better (AUROC > 0.892) when compared with other methods in the literature (AUROC < 0.867). The introduction of the denoising step further improved the algorithm performance. The segmentation sensitivity, specificity and accuracy were 0.612, 0.933 and 0.895, respectively. Results from the processing of one test image are illustrated in Fig. 1.

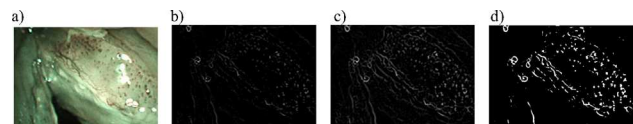


Fig. 1 Original laryngeal image (a). Vessel enhancement for $\sigma = 1.3$ (b) and 1.5 (c). Vessel segmentation result (d)

Conclusion

In this work, a fully automatic laryngeal vessel segmentation algorithm has been proposed. The anisotropic nature of the implemented denoising algorithm proved to be effective to face the noisy nature of endoscopic images while enhancing meaningful features. This was demonstrated by the higher performance reached in the subsequent vessel segmentation phase. The proposed multi-scale vessel enhancement algorithm outperformed other methods presented in literature in terms of area under the ROC curve, being able to segment both healthy tubular-like vessels and pathological blob-like vessels. In addition, these results demonstrate the benefits of the SVM method used, showing it was able to efficiently model the complexity of endoscopic images in terms of noise, non-uniform illumination and non-constant vesselness measure. Future developments will focus on improving the classification algorithm through an enlarged training and evaluation dataset, which will include a wider range of laryngeal pathologies.

References

- [1] Lukes P, Zabrodsky M, Lukesova E, Chovanec M, Astl J, Betka J A, Plzak J (2014) The role of nbi hdtv magnifying endoscopy in the prehistologic diagnosis of laryngeal papillomatosis and spinocellular cancer. *BioMed research international*.
- [2] Mendrik A M, Vonken E, Rutten A, Viergever M A, Van Ginneken B (2009) Noise reduction in computed tomography